



**Homoleptic versus heteroleptic trinuclear systems with mixed L-cysteinate and D-penicillamine regulated by a diphosphine linker**

Journal:	<i>Dalton Transactions</i>
Manuscript ID	DT-ART-02-2020-000440.R1
Article Type:	Paper
Date Submitted by the Author:	17-Feb-2020
Complete List of Authors:	Hanprasit, Sasikarn; Osaka University, Department of Chemistry, Graduate School of Science Yoshinari, Nobuto; Osaka University, Department of Chemistry, Graduate School of Science Saito, Daisuke; Hokkaido University, Chemistry Kato, Masako; Hokkaido University, Chemistry Konno, Takumi; Osaka University, Department of Chemistry, Graduate School of Science

## ARTICLE

## Homoleptic versus heteroleptic trinuclear systems with mixed L-cysteinate and D-penicillamate regulated by a diphosphine linker

Received 00th January 20xx,  
Accepted 00th January 20xx

DOI: 10.1039/x0xx00000x

Sasikarn Hanprasit,<sup>a</sup> Nobuto Yoshinari,<sup>a</sup> Daisuke Saito,<sup>b</sup> Masako Kato,<sup>b</sup> and Takumi Konno<sup>\*a</sup>

Controlled generation of homoleptic versus heteroleptic Au<sub>2</sub>M (M = Ni<sup>II</sup>, Zn<sup>II</sup>) trinuclear complexes, which is achieved by a slight change in the diphosphine P<sup>AP</sup> linker of digold(I) metalloligands, [Au<sub>2</sub>(P<sup>AP</sup>)(D-pen)<sub>2</sub>]<sup>2-</sup> (L1<sup>P<sup>AP</sup></sup>; D-pen = D-penicillamate) and [Au<sub>2</sub>(P<sup>AP</sup>)(L-cys)<sub>2</sub>]<sup>2-</sup> (L2<sup>P<sup>AP</sup></sup>; L-cys = L-cysteinate), is reported. The reactions of a 1:1 mixture of L1<sup>dppm</sup> and L2<sup>dppm</sup> (dppm = bis(diphenylphosphino)methane) with M = Ni<sup>II</sup>, Zn<sup>II</sup> gave the homoleptic Au<sub>2</sub>M complexes, [M(L1<sup>dppm</sup>)] and [M(L2<sup>dppm</sup>)], which co-crystallized to form [M(L1<sup>dppm</sup>)]·[M(L2<sup>dppm</sup>)] (**1<sub>M</sub>**). Similar reactions using L1<sup>dppe</sup> and L2<sup>dppe</sup> (dppe = bis(diphenylphosphino)ethane), instead of L1<sup>dppm</sup> and L2<sup>dppm</sup>, led to the selective production and crystallization of the heteroleptic Au<sub>2</sub>M complex, [M(L3<sup>dppe</sup>)] (**2<sub>M</sub>**; L3<sup>dppe</sup> = [Au<sub>2</sub>(dppe)(L-cys)(D-pen)]<sup>2-</sup>), accompanied by the scrambling of L1<sup>dppe</sup> and L2<sup>dppe</sup>. The homoleptic **1<sub>M</sub>** and the heteroleptic **2<sub>M</sub>** showed different absorption (green versus blue) and emission (yellow versus orange) colours for M = Ni<sup>II</sup> and Zn<sup>II</sup>, respectively.

### Introduction

Self-assembly of multinuclear and supramolecular coordination compounds from metal ions and multidentate ligands continues to attract considerable interest because of the fascinating functionalities and structural diversities of these compounds.<sup>1-3</sup> This class of compounds was initially synthesized as 'homoleptic' species that consist of a single kind of ligand.<sup>2</sup> In recent years, the focus has shifted from 'homoleptic' species to 'heteroleptic' ones that contain two different kinds of multidentate ligands in one molecule, with the aim of creating more diverse structures with different physical and chemical properties, as well as practical functionalities.<sup>3,4</sup> Indeed, noticeable differences in photophysical,<sup>5</sup> guest-encapsulation,<sup>6,7</sup> catalytic,<sup>8</sup> and magnetic properties<sup>9</sup> have been recognized between homoleptic and heteroleptic compounds in some coordination systems. To date, several synthetic strategies, such as the design of sterically and topologically controlled ligands,<sup>10,11</sup> the use of geometrically controlled metal centres,<sup>12</sup> the thermodynamic control of molecular formations,<sup>7</sup> and selective precipitation upon crystallization,<sup>13</sup> have been applied for the independent generation of homoleptic and heteroleptic coordination compounds. However, the rational control of homoleptic versus heteroleptic species from two

different kinds of ligands is still a great challenge in this research field.

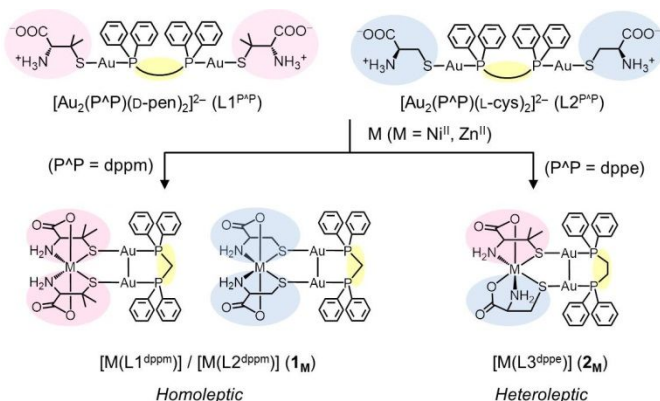
As part of our long-standing study on the stepwise preparation of heterometallic coordination compounds based on metalloligands with thiol-containing amino acids,<sup>14,15</sup> we have designed and synthesized digold(I) metalloligands, [Au<sub>2</sub>(P<sup>AP</sup>)(D-pen)<sub>2</sub>]<sup>2-</sup> (L1<sup>P<sup>AP</sup></sup>) with linking diphosphine P<sup>AP</sup> and terminal D-pen (D-penicillamate) ligands.<sup>15</sup> Previously, we reported that the Au<sub>2</sub>Ni<sup>II</sup> trinuclear structure in [Ni(L1<sup>dppm</sup>)] with an 8-membered metalloring is extended to a Au<sub>4</sub>Ni<sup>II</sup><sub>2</sub> hexanuclear structure in [Ni<sub>2</sub>(L1<sup>dppe</sup>)<sub>2</sub>] with an 18-membered metalloring by changing the P<sup>AP</sup> ligand in L1<sup>P<sup>AP</sup></sup> from dppm (bis(diphenylphosphino)methane) to dppe (1,2-bis(diphenylphosphino)ethane).<sup>16,17</sup> To determine whether a similar change in metalloring size occurs for another coordination system, we tried to prepare Au<sup>I</sup>-Ni<sup>II</sup> multinuclear complexes using analogous digold(I) metalloligands [Au<sub>2</sub>(P<sup>AP</sup>)(L-cys)<sub>2</sub>]<sup>2-</sup> (L2<sup>P<sup>AP</sup></sup>, P<sup>AP</sup> = dppm, dppe) with L-cys (L-cysteinate) instead of D-pen. Unfortunately, the reaction of L2<sup>P<sup>AP</sup></sup> with Ni<sup>2+</sup> resulted in the precipitation of unidentified solids. However, the use of a 1:1 mixture of L1<sup>P<sup>AP</sup></sup> and L2<sup>P<sup>AP</sup></sup> for the reaction with Ni<sup>2+</sup> afforded well-characterized crystalline products. We found that not only the product obtained from L1<sup>dppm</sup> and L2<sup>dppm</sup> (**1<sub>Ni</sub>**) but also the product from L1<sup>dppe</sup> and L2<sup>dppe</sup> (**2<sub>Ni</sub>**) has a Au<sub>2</sub>Ni<sup>II</sup> trinuclear structure with an 8-membered ring. Remarkably, **1<sub>Ni</sub>** was found to be a 1:1 mixture of homoleptic [Ni(L1<sup>dppm</sup>)] and [Ni(L2<sup>dppm</sup>)] complexes, whereas **2<sub>Ni</sub>** has a heteroleptic structure in [Ni(L3<sup>dppe</sup>)], where L3<sup>dppe</sup> is [Au<sub>2</sub>(dppe)(L-cys)(D-pen)]<sup>2-</sup> containing both L-cys and D-pen ligands (Scheme 1). This was also the case for the reactions with Zn<sup>2+</sup>, yielding only a 1:1 mixture of [Zn(L1<sup>dppm</sup>)] and [Zn(L2<sup>dppm</sup>)] (**1<sub>Zn</sub>**) from L1<sup>dppm</sup> and L2<sup>dppm</sup>, whereas [Zn(L3<sup>dppe</sup>)] (**2<sub>Zn</sub>**) was exclusively obtained from L1<sup>dppe</sup> and L2<sup>dppe</sup>. To our knowledge, such a selective generation

<sup>a</sup> Department of Chemistry, Graduate School of Science, Osaka University, Toyonaka, Osaka 560-0043, Japan. E-mail: konno@chem.sci.osaka-u.ac.jp; Tel: +81-6-6850-5765

<sup>b</sup> Department of Chemistry, Faculty of Science, Hokkaido University, Sapporo, Hokkaido 060-0810, Japan.

† Electronic supplementary information (ESI) available: Synthesis, diffuse reflection, IR, powder X-ray diffraction and crystallographic data. CCDC 1972832-1972835. For ESI and crystallographic data in CIF or other electronic format see DOI: 10.1039/x0xx00000x

of homoleptic versus heteroleptic species via the slight modification of an ancillary ligand is unprecedented. The differences in spectroscopic characteristics between the homoleptic and heteroleptic systems are also reported.



**Scheme 1.** Synthesis of homoleptic and heteroleptic  $Au_2M$  trinuclear complexes ( $1_M$  and  $2_M$ ) from a mixture of  $L1^{P^{AP}}$  and  $L2^{P^{AP}}$ .

## Results and discussion

### Synthesis and characterization of $1_{Ni}$

The digold(I) metalloligands with dppm,  $[Au_2(dppm)(D-pen)_2]^{2-}$  ( $L1^{dppm}$ ) and  $[Au_2(dppm)(L-cys)_2]^{2-}$  ( $L2^{dppm}$ ), were prepared *in situ* from the reactions of  $[Au_2Cl_2(dppm)]^{18}$  with D-H<sub>2</sub>pen or L-H<sub>2</sub>cys in a 1:2 ratio in EtOH/H<sub>2</sub>O under basic conditions. The formation of  $L1^{dppm}$  and  $L2^{dppm}$  was confirmed by the ESI-TOF mass spectra, which exhibit a dominant signal at  $m/z = 1097$  corresponding to  $\{[Au_2(dppm)(D-pen)_2] + Na\}^+$  for  $L1^{dppm}$  and at  $m/z = 1041$  corresponding to  $\{[Au_2(dppm)(L-cys)_2] + Na\}^+$  for  $L2^{dppm}$  (Fig. S1, ESI<sup>†</sup>). Subsequently, nickel(II) acetate was treated with a solution containing  $L1^{dppm}$  and  $L2^{dppm}$  in a 1:1 ratio, which gave a green solution. Slow evaporation of the reaction solution afforded green needle-like crystals ( $1_{Ni}$ ) in a satisfactory yield (51 %). The CHN elemental and X-ray fluorescence analyses implied that  $1_{Ni}$  contains  $Ni^{2+}$ ,  $L1^{dppm}$  and  $L2^{dppm}$  in a 2:1:1 ratio. The absorption spectrum of  $1_{Ni}$  showed a visible d-d band at 589 nm and a broad d-d band in the near-IR region (Fig. S2, ESI<sup>†</sup>). These spectral features are very similar to those of the previously reported  $[Ni(L1^{dppm})]$ .<sup>16</sup> Unlike  $[Ni(L1^{dppm})]$ , however,  $1_{Ni}$  is almost CD silent in this region, consistent with the presence of  $L1^{dppm}$  and  $L2^{dppm}$  in a 1:1 ratio.

Single-crystal X-ray analysis revealed that  $1_{Ni}$  contains the two homoleptic  $Au_2Ni^{II}$  trinuclear molecules,  $[Ni\{Au_2(dppm)(D-pen)_2\}]$  ( $[Ni(L1^{dppm})]$ ) and  $[Ni\{Au_2(dppm)(L-cys)_2\}]$  ( $[Ni(L2^{dppm})]$ ), in an asymmetric unit (Fig. 1a). The molecular structure of  $[Ni(L1^{dppm})]$  in  $1_{Ni}$  is essentially the same as that of the previously reported  $[Ni(L1^{dppm})]$ ;<sup>16</sup>  $L1^{dppm}$  chelates to a  $Ni^{II}$  centre in a hexadentate- $N_2, O_2, S_2$  fashion to form a *cis(N)·trans(O)·cis(S)*- $[Ni(D-pen)_2]^{2-}$  octahedral unit with an 8-membered  $Au_2Ni^{II}$  metalloring.<sup>19</sup> The other molecule  $[Ni(L2^{dppm})]$ , which has L-cys instead of D-pen, shows the same structural feature as  $[Ni(L1^{dppm})]$ ; the *cis(N)·trans(O)·cis(S)*- $[Ni(D-pen)_2]^{2-}$  octahedral unit with an 8-membered metalloring is formed by coordination

of  $L2^{dppm}$  in a hexadentate- $N_2, O_2, S_2$  fashion.<sup>19</sup> The Au...Au distances in  $[Ni(L1^{dppm})]$  and  $[Ni(L2^{dppm})]$  are 3.1769(17) Å and 3.1841(19) Å, respectively, suggesting the presence of an aurophilic interaction in each molecule.<sup>18,20</sup> In the crystal structure, the  $[Ni(L1^{dppm})]$  and  $[Ni(L2^{dppm})]$  molecules are alternately arranged to construct a 2D layer structure through H-bonding (av  $N\cdots O = 3.20$  Å) and  $CH\cdots\pi$  (av  $C\cdots C = 3.68$  Å) interactions (Fig. S3, ESI<sup>†</sup>). The powder X-ray diffraction (PXRD) pattern of the bulk sample of  $1_{Ni}$  matches well with the pattern simulated from the single-crystal X-ray data (Fig. S4, ESI<sup>†</sup>). This implies that only homoleptic  $1_{Ni}$  was produced from  $L1^{dppm}$ ,  $L2^{dppm}$  and  $Ni^{2+}$  upon crystallization.

### Synthesis and characterization of $2_{Ni}$

The analogous metalloligands containing dppe instead of dppm,  $[Au_2(dppe)(D-pen)_2]^{2-}$  ( $L1^{dppe}$ ) and  $[Au_2(dppe)(L-cys)_2]^{2-}$  ( $L2^{dppe}$ ), were also prepared *in situ* using  $[Au_2Cl_2(dppe)]^{21}$  instead of  $[Au_2Cl_2(dppm)]$  and were characterized by ESI-TOF mass spectrometry (Fig. S5, ESI<sup>†</sup>). Similar treatment of nickel(II) acetate with a 1:1 mixture of  $L1^{dppe}$  and  $L2^{dppe}$  yielded a pale blue solution. From this reaction solution, blue plate-like crystals ( $2_{Ni}$ ) that are sparingly soluble in any solvent were isolated (yield: 58 %). The elemental and X-ray fluorescence analytical data were in agreement with a formula that contains  $Ni^{2+}$ ,  $L1^{dppe}$  and  $L2^{dppe}$  in a 2:1:1 ratio, as in the case of  $1_{Ni}$ . However, the single-crystal X-ray analysis demonstrated that  $2_{Ni}$  is not a 1:1 mixture of the homoleptic  $[Ni(L1^{dppe})]$  and  $[Ni(L2^{dppe})]$  but is unexpectedly heteroleptic  $[Ni(L3^{dppe})]$ , in which a  $Ni^{II}$  centre is surrounded by the digold(I) metalloligand with both D-pen and L-cys ( $L3^{dppe} = [Au_2(dppe)(D-pen)(L-cys)]^{2-}$ ), forming a 9-membered metalloring with an average Au...Au distance of 2.97 Å (Fig. 1b). Thus, metalloligand scrambling between  $L1^{dppe}$  and  $L2^{dppe}$  occurred in the course of the reactions, accompanied by cleavage of the Au-P or Au-S bonds in  $L1^{dppe}$  and  $L2^{dppe}$ .<sup>22</sup> The asymmetric unit of  $2_{Ni}$  contains two independent  $[Ni(L3^{dppe})]$  molecules with a *cis(N)·cis(O)·cis(S)* configurational  $[Ni(D-pen)(L-cys)]^{2-}$  unit; the two molecules are discriminated by the chirality at the  $Ni^{II}$  centre, C (clockwise) and A (anti-clockwise), arising from the arrangement of two N, two O and two S donor atoms.<sup>19</sup> In the crystal structure, the C and A diastereomers are alternately connected by H-bonding (av  $N\cdots O = 2.95$  Å) and  $CH\cdots\pi$  (av  $C\cdots C = 3.74$  Å) interactions, constructing a 2D structure that is similar to that found in  $1_{Ni}$  (Fig. S6, ESI<sup>†</sup>). The selective generation of heteroleptic  $2_{Ni}$  upon crystallization was evidenced by PXRD studies (Fig. S7, ESI<sup>†</sup>). It should be noted that heteroleptic  $2_{Ni}$  is blue in colour, which differs from the green colour of homoleptic  $1_{Ni}$ . Indeed, the diffuse reflection spectrum of  $2_{Ni}$  in the solid state showed a visible d-d band at 571 nm, which is higher in energy than the corresponding band at 589 nm for  $1_{Ni}$  (Fig. 2). This is explained by the difference in the splitting energy of the d-d band between the *cis(N)·trans(O)·cis(S)* configurational  $Ni^{II}$  centre in  $1_{Ni}$  and the *cis(N)·cis(O)·cis(S)* configurational centre in  $2_{Ni}$ . A similar absorption energy difference has been observed between *cis(N)trans(O)cis(S)*- $[Co(D-pen)_2]^-$  and *cis(N)cis(O)cis(S)*- $[Co(D-pen)(L-pen)]^-$ .<sup>23</sup>

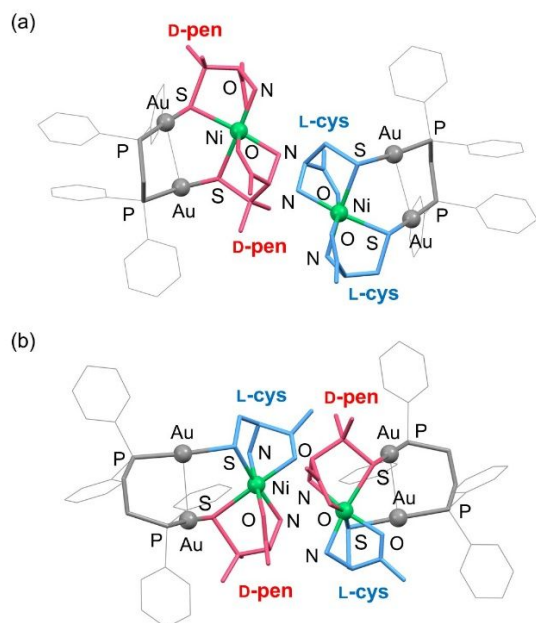


**Fig. 1.** Perspective views of (a) the homoleptic molecules, (left)  $[\text{Ni}(\text{L1}^{\text{dppm}})]$  and (right)  $[\text{Ni}(\text{L2}^{\text{dppm}})]$ , in  $\mathbf{1}_{\text{Ni}}$  and (b) the heteroleptic molecules, (left) A- $[\text{Ni}(\text{L3}^{\text{dppe}})]$  and (right) C- $[\text{Ni}(\text{L3}^{\text{dppe}})]$ , in  $\mathbf{2}_{\text{Ni}}$ .

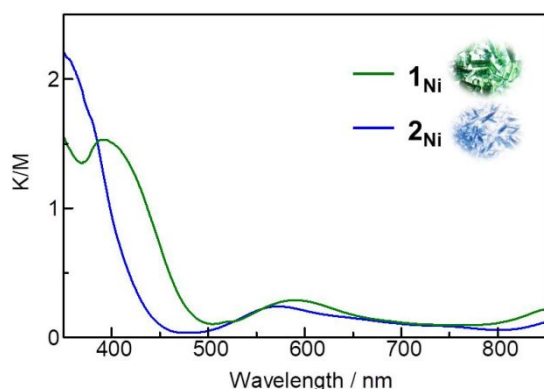


**Fig. 2.** Diffuse reflectance spectra of  $\mathbf{1}_{\text{Ni}}$  (green) and  $\mathbf{2}_{\text{Ni}}$  (blue). Inset: photographs of the samples.

### Synthesis and characterization of $\mathbf{1}_{\text{Zn}}$ and $\mathbf{2}_{\text{Zn}}$

We also carried out reactions of a 1:1 mixture of  $\text{L1}^{\text{P}^{\text{NP}}}$  and  $\text{L2}^{\text{P}^{\text{NP}}}$  using zinc(II) acetate. The reactions yielded homoleptic  $\mathbf{1}_{\text{Zn}}$  consisting of  $[\text{Zn}(\text{L1}^{\text{dppm}})]$  and  $[\text{Zn}(\text{L2}^{\text{dppm}})]$  in a 1:1 ratio and heteroleptic  $\mathbf{2}_{\text{Zn}}$  containing only  $[\text{Zn}(\text{L3}^{\text{dppe}})]$  as colourless crystals for the dppe and the dppe systems, respectively, similar to the reactions with nickel(II) acetate. The assignment of  $\mathbf{1}_{\text{Zn}}$  and  $\mathbf{2}_{\text{Zn}}$  was made by elemental and X-ray fluorescence analyses. The single-crystal X-ray analyses established that the structures of homoleptic  $\mathbf{1}_{\text{Zn}}$  and heteroleptic  $\mathbf{2}_{\text{Zn}}$  correspond well with those of  $\mathbf{1}_{\text{Ni}}$  and  $\mathbf{2}_{\text{Ni}}$ , respectively, except for the presence of  $\text{Zn}^{\text{II}}$  in place of  $\text{Ni}^{\text{II}}$  (Figs. 3, S8, S9, ESI<sup>†</sup>). The powder X-ray diffraction studies implied that  $\mathbf{1}_{\text{Zn}}$  and  $\mathbf{2}_{\text{Zn}}$  were selectively produced upon crystallization in the dppe and dppe systems, respectively, as in the case of  $\mathbf{1}_{\text{Ni}}$  and  $\mathbf{2}_{\text{Ni}}$  (Figs. S10, S11, ESI<sup>†</sup>). Notably, different emission colours were observed for  $\mathbf{1}_{\text{Zn}}$  and  $\mathbf{2}_{\text{Zn}}$  at room temperature;  $\mathbf{1}_{\text{Zn}}$  displayed yellow emission, whereas  $\mathbf{2}_{\text{Zn}}$

showed orange emission. As shown in Fig 4, the emission spectra of  $\mathbf{1}_{\text{Zn}}$  and  $\mathbf{2}_{\text{Zn}}$  give a broad band at 516 nm and 525 nm, with similar quantum yields of  $\Phi = 0.04$  and 0.05, respectively (Fig. 4, Table S1, ESI<sup>†</sup>). The origin of the emissions was tentatively assigned to phosphorescence arising primarily from a  $^3\text{LMMCT} (\text{S} \rightarrow \text{Au} \cdots \text{Au})$  transition,<sup>24</sup> consistent with the emission lifetimes on the order of microseconds (Table S1, ESI<sup>†</sup>). The difference in the average Au...Au separations (3.17 Å for  $\mathbf{1}_{\text{Zn}}$  versus 2.99 Å for  $\mathbf{2}_{\text{Zn}}$ ) may be responsible for the difference in emission energies in the present systems.

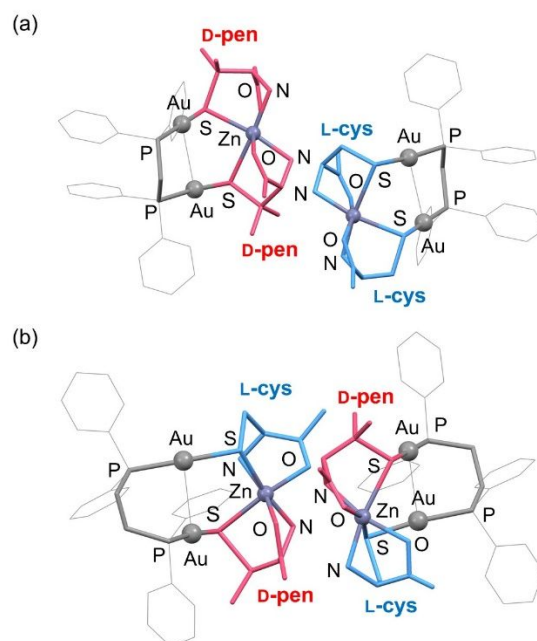


**Fig. 3.** Perspective views of (a) the homoleptic molecules, (left)  $[\text{Zn}(\text{L1}^{\text{dppm}})]$  and (right)  $[\text{Zn}(\text{L2}^{\text{dppm}})]$ , in  $\mathbf{1}_{\text{Zn}}$  and (b) the heteroleptic molecule, (left) A- $[\text{Zn}(\text{L3}^{\text{dppe}})]$  and (right) C- $[\text{Zn}(\text{L3}^{\text{dppe}})]$ , in  $\mathbf{2}_{\text{Zn}}$ .

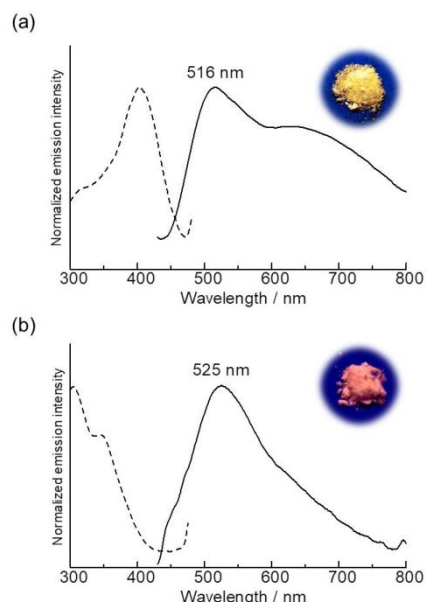


**Fig. 4.** Emission (solid line) and excitation (dashed line) spectra of (a)  $\mathbf{1}_{\text{Zn}}$  ( $\lambda_{\text{ex}} = 400 \text{ nm}$ ,  $\lambda_{\text{em}} = 520 \text{ nm}$ ) and (b)  $\mathbf{2}_{\text{Zn}}$  ( $\lambda_{\text{ex}} = 400 \text{ nm}$ ,  $\lambda_{\text{em}} = 510 \text{ nm}$ ) in the solid state at room temperature. Inset: photographs of  $\mathbf{1}_{\text{Zn}}$  and  $\mathbf{2}_{\text{Zn}}$  under UV-light irradiation ( $\lambda = 365 \text{ nm}$ ).

### Formation and crystallization of $\mathbf{1_M}$ and $\mathbf{2_M}$

To identify the species formed in the reaction solutions, the ESI mass spectra of the solutions after reacting  $L1^{P^AP}$ ,  $L2^{P^AP}$  and  $M = Ni^{2+}$ ,  $Zn^{2+}$  for 1 h were measured. The ESI mass spectrum of the reaction solution for  $P^AP = dppm$  gave two main signals corresponding to the homoleptic  $[M(L1^{dppm})]$  and heteroleptic  $[M(L3^{dppm})]$  species (Figs. 5, S12, ESI<sup>†</sup>). Another signal corresponding to  $[M(L2^{dppm})]$  was also observed, although its intensity was quite low, presumably due to the poor ionization of this species. Considering that the statistical formation ratio of  $[M(L1^{P^AP})]$ ,  $[M(L2^{P^AP})]$  and  $[M(L3^{P^AP})]$  from the scrambling of a 1:1 mixture of  $L1^{P^AP}$  and  $L2^{P^AP}$  is 1:1:2 and that the signal for  $[M(L1^{dppm})]$  is more intense than that for  $[M(L3^{dppm})]$ , it is assumed that the homoleptic species,  $[M(L1^{dppm})]$  and  $[M(L2^{dppm})]$ , were preferentially formed in the reaction and that these species were selectively crystallized as  $\mathbf{1_M}$  because their solubility was lower than that of the heteroleptic species  $[M(L3^{dppm})]$ . On the other hand, only a dominant signal due to

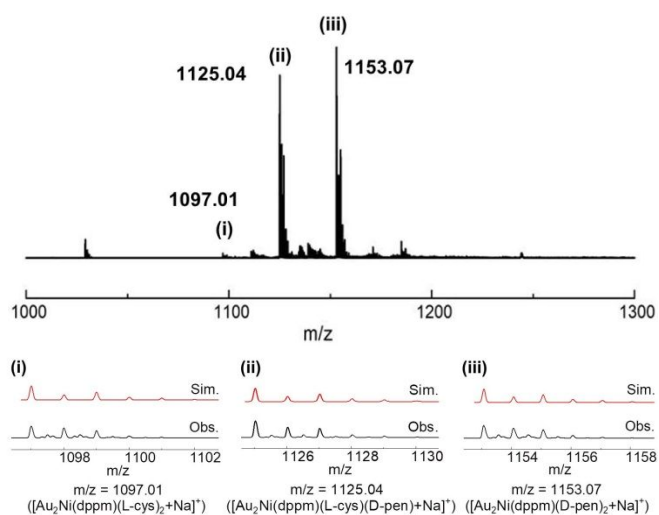


**Fig. 5.** ESI mass spectra of the reaction mixture of  $L1^{dppm}$ ,  $L2^{dppm}$  and nickel acetate in methanol-water (1:1): (i)  $[Ni\{Au_2(dppm)(L-cys)_2\} + Na]^+$  ( $m/z = 1097.01$ ), (ii)  $[Ni\{Au_2(dppm)(L-cys)(D-pen)\} + Na]^+$  ( $m/z = 1125.04$ ) and (iii)  $[Ni\{Au_2(dppm)(D-pen)_2\} + Na]^+$  ( $m/z = 1153.07$ ).

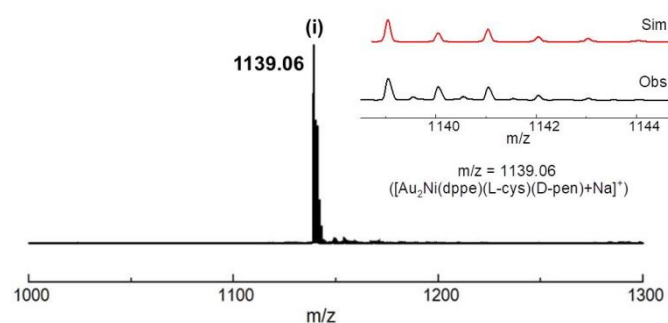


**Fig. 6.** ESI mass spectra of the reaction mixture of  $L1^{dppe}$ ,  $L2^{dppe}$  and nickel acetate in methanol-water (1:1): (i)  $[Ni\{Au_2(dppe)(L-cys)(D-pen)\} + Na]^+$  ( $m/z = 1139.06$ ).

the heteroleptic  $[M(L3^{dppm})]$  species was observed in the ESI mass spectrum of the reaction solution for the  $dppe$  system; signals corresponding to the homoleptic  $[M(L1^{dppe})]$  and  $[M(L2^{dppe})]$  species were not observed (Figs. 6, S13, ESI<sup>†</sup>). This is indicative of the selective formation of the heteroleptic  $[M(L3^{dppm})]$  in the reactions of the  $dppe$  system.

Molecular model examinations revealed that a pair of P-Au bonds are nearly parallel in the  $[Au_2(dppm)]^{2+}$  moiety when the Au...Au separation is maintained to form an aurophilic interaction (Fig. 7). On the other hand, a pair of P-Au bonds must be highly skewed in the  $[Au_2(dppe)]^{2+}$  moieties to maintain the Au...Au separation. This structural difference has been observed in the X-ray structures of  $[Au_2Cl_2(dppm)]$  and  $[Au_2Cl_2(dppe)]$ .<sup>18,20,21</sup> For the  $[M(\text{tridentate-N,O,S})_2]$  unit, the direction of a pair of lone pairs from two thiolato atoms is nearly parallel in the *cis(N)·trans(O)·cis(S)* configuration, whereas the direction is highly skewed in the *cis(N)·cis(O)·cis(S)* configuration (Fig. 8). In fact, the torsion angles of S–Au...Au–S in  $\mathbf{2_{Ni}}$  (av 59.8°) and  $\mathbf{2_{Zn}}$  (av 61.9°) are much larger than those in  $\mathbf{1_{Ni}}$  (av 17.4°) and  $\mathbf{1_{Zn}}$  (av 17.8°). Thus, the best matching of the directionality between a pair of P-Au bonds and a pair of lone pair electrons accounts for the preferential/selective formation of  $\mathbf{1_M}/\mathbf{2_M}$ . Consistent with this finding, the DFT calculations for the Zn<sup>II</sup> system indicated that  $[Zn(L3^{dppm})]$  has a total molecular energy higher than that of  $[Zn(L1^{dppm})]/[Zn(L2^{dppm})]$ , whereas  $[Zn(L1^{dppe})]/[Zn(L2^{dppe})]$  has a molecular energy higher than that of  $[Zn(L3^{dppe})]$  (Table S2, ESI<sup>†</sup>).

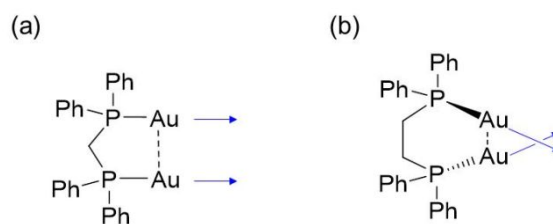


**Fig. 7.** Schematic illustration of the directions of P-Au lines in (a)  $[Au_2(dppm)]^{2+}$  and (b)  $[Au_2(dppe)]^{2+}$ .

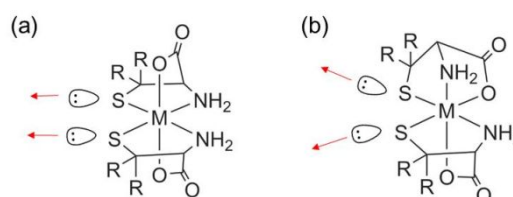


**Fig. 8.** Schematic illustration of the directions of lone pairs on S atoms in (a) *cis(N)trans(O)cis(S)*- $[M(L-cys \text{ or } D-pen)_2]^{2-}$  and (b) *cis(N)cis(O)cis(S)*- $[M(L-cys)(D-pen)]^{2-}$ .

## Experimental

### Preparation of the homoleptic $[M\{Au_2(dppm)(D-pen)_2\} \cdot [M\{Au_2(dppm)(L-cys)_2\}]$ ( $\mathbf{1_M}$ ; $M = Ni^{II}, Zn^{II}$ ).

To a white suspension containing 0.051 g (0.06 mmol) of  $[Au_2Cl_2(dppm)]$ <sup>18</sup> in ethanol/water (3 mL/3 mL) was added a colourless solution containing 0.017 g (0.14 mmol) of L-H<sub>2</sub>cys in

0.5 M aqueous NaOH (0.5 mL), which gave a colourless solution (**A**). In a different vial, to a white suspension containing 0.051 g (0.06 mmol) of  $[\text{Au}_2\text{Cl}_2(\text{dppm})]$  in ethanol/water (3 mL/3 mL) was added a colourless solution containing 0.022 g (0.15 mmol) of D-H<sub>2</sub>pen in 0.5 M aqueous NaOH (0.33 mL), which gave a colourless solution (**B**). The ESI-mass spectra indicated the formation of the digold(I) metalloligands  $[\text{Au}_2(\text{dppm})(\text{L-cys})_2]^{2-}$  and  $[\text{Au}_2(\text{dppm})(\text{D-pen})_2]^{2-}$  in the colourless solutions **A** and **B**, respectively (Fig. S1, ESI<sup>†</sup>). The two colourless solutions **A** and **B** were mixed, followed by the addition of 0.030 g (0.12 mmol) of  $\text{Ni}(\text{OAc})_2 \cdot 4\text{H}_2\text{O}$ . After stirring the mixture at room temperature for 1 h, the resulting green solution was slowly evaporated at room temperature, which gave green crystals together with a small amount of an oily product. The products were recrystallized from MeOH/EtOH (1:1) to give green plate-like crystals (**1<sub>Ni</sub>**). Yield: 0.038 g (51%). Anal. Calcd for  $[\text{Ni}\{\text{Au}_2(\text{dppm})(\text{L-cys})_2\}][\text{Ni}\{\text{Au}_2(\text{dppm})(\text{D-pen})_2\}] \cdot 12\text{H}_2\text{O}$  =  $\text{C}_{66}\text{H}_{96}\text{N}_4\text{Au}_4\text{Ni}_2\text{O}_{20}\text{P}_4\text{S}_4$ : C, 32.72; H, 3.99; N, 2.31%. Found: C, 32.99; H, 4.02; N, 2.06%. IR spectrum ( $\text{cm}^{-1}$ , ATR): 1585 ( $\nu_{\text{COO}^-}$ ), 1436 ( $\nu_{\text{P-Ph}}$ ), 746-695 ( $\nu_{\text{Ph}}$ ).

#### Preparation of the heteroleptic $[\text{M}\{\text{Au}_2(\text{dppe})(\text{L-cys})(\text{D-pen})\}]$ (**2<sub>M</sub>**; M = Ni<sup>II</sup>, Zn<sup>II</sup>).

To a white suspension containing 0.052 g (0.06 mmol) of  $[\text{Au}_2\text{Cl}_2(\text{dppe})]^{2+}$  in MeOH (6 mL) was added a colourless solution containing 0.017 g (0.14 mmol) of L-H<sub>2</sub>cys in 0.5 M aqueous NaOH, which gave a colourless solution (**C**). In a different vial, to a white suspension containing 0.052 g (0.06 mmol) of  $[\text{Au}_2\text{Cl}_2(\text{dppe})]$  in MeOH (6 mL) was added a colourless solution containing 0.022 g (0.15 mmol) of D-H<sub>2</sub>pen in 0.5 M aqueous NaOH (0.33 mL), which gave a colourless solution (**D**). The ESI-mass spectra indicated the formation of the digold(I) metalloligands  $[\text{Au}_2(\text{dppe})(\text{L-cys})_2]^{2-}$  and  $[\text{Au}_2(\text{dppe})(\text{D-pen})_2]^{2-}$  in the colourless solutions **C** and **D**, respectively (Fig. S5, ESI<sup>†</sup>). The two colourless solutions **C** and **D** were mixed, followed by the addition of 0.030 g (0.12 mmol) of  $\text{Ni}(\text{OAc})_2 \cdot 4\text{H}_2\text{O}$ . After stirring the mixture at room temperature for 1 h, the resulting pale blue solution was slowly evaporated at room temperature, which gave blue plate crystals (**2<sub>Ni</sub>**) in a smoky solution. After decantation, the crystals were collected by filtration and then washed with water. Yield: 0.044 g (58%). Anal. Calcd for  $[\text{Ni}\{\text{Au}_2(\text{dppe})(\text{L-cys})(\text{D-pen})\}] \cdot 7\text{H}_2\text{O}$  =  $\text{C}_{34}\text{H}_{52}\text{N}_2\text{Au}_2\text{NiO}_{11}\text{P}_2\text{S}_2$ : C, 32.81; H, 4.29; N, 2.25%. Found: C, 32.70; H, 4.29; N, 2.20%. IR spectrum ( $\text{cm}^{-1}$ , ATR): 1586 ( $\nu_{\text{COO}^-}$ ), 1435 ( $\nu_{\text{P-Ph}}$ ) and 745-693 ( $\nu_{\text{Ph}}$ ).

A similar reaction using  $\text{Zn}(\text{OAc})_2 \cdot 2\text{H}_2\text{O}$  instead of  $\text{Ni}(\text{OAc})_2 \cdot 4\text{H}_2\text{O}$  gave colourless plate-like crystals (**2<sub>Zn</sub>**). Yield: 0.046 g (57%). Anal. Calcd for  $[\text{Zn}\{\text{Au}_2(\text{dppe})(\text{L-cys})(\text{D-pen})\}] \cdot 9\text{H}_2\text{O}$  =  $\text{C}_{34}\text{H}_{56}\text{N}_2\text{Au}_2\text{ZnO}_{13}\text{P}_2\text{S}_2$ : C, 31.75; H, 4.39; N, 2.18%. Found: C, 31.65; H, 4.41; N, 2.23%. IR spectrum ( $\text{cm}^{-1}$ , ATR): 1610 ( $\nu_{\text{COO}^-}$ ), 1436 ( $\nu_{\text{P-Ph}}$ ) and 743-693 ( $\nu_{\text{Ph}}$ ).

#### Physical Measurements.

Elemental analyses (C, H, N) were performed at Osaka University with YANACO CHN coder MT-5 or MT-6. The absorption spectra were recorded on a JASCO V-570

spectrophotometer. The diffuse reflectance spectra were recorded on a JASCO V-570 spectrophotometer using  $\text{MgSO}_4$ . X-ray fluorescence spectrometry was performed on a SHIMADZU EDX-7000 spectrometer. The powder X-ray diffraction patterns were recorded at a controlled temperature in transmission mode [synchrotron radiation  $\lambda = 1.0 \text{ \AA}$ ;  $2\theta$  range =  $2-78^\circ$ ; step width =  $0.01^\circ$ ; data collection time = 1 min] on a diffractometer equipped with a MYTHEN microstrip X-ray detector (Dectris Ltd.) at the SPring-8 BL02B2 beamline. The crystals were loaded into a glass capillary tube (diameter = 0.3 mm), which was rotated during the measurements. The simulated powder X-ray diffraction patterns were generated based on the single-crystal X-ray structural data using Mercury 3.9 software. The electrospray ionization time-of-flight (ESI-TOF) mass spectra were recorded on a BRUKER micrOTOF II-OS in  $\text{H}_2\text{O}/\text{CH}_3\text{OH}$ . Sample concentrations were set to 10  $\mu\text{M}$  and measured in positive mode. The luminescence spectra were recorded with a JASCO FP-8600 spectrometer at room temperature in the solid states using a Xe lamp as the light source. The internal emission quantum yields ( $\Phi$ ) were obtained via the absolute measuring method using an integrating sphere unit (Hamamatsu C9920-02 Absolute PL Quantum Yield Measurement System). Emission lifetime measurements were recorded using a Hamamatsu Quantaaurus-Tau C11367 system using an LED light source (405 nm) for excitation. The emission decays were analyzed using three exponentials;  $I = A_1\exp(-t/\tau_1) + A_2\exp(-t/\tau_2) + A_3\exp(-t/\tau_3)$ , where  $A_i$  denotes the pre-exponential factors for lifetimes  $\tau_i$ . The average emission lifetimes ( $\tau_{\text{ave}}$ ) were calculated using the following equation (1):

$$\tau_{\text{ave}} = \frac{\sum A_i \tau_i^2}{\sum A_i \tau_i} \quad (1)$$

#### Computational study.

DFT calculations were performed with the Gaussian 09 program<sup>25</sup> at the B3LYP<sup>26</sup> level using a Lan12DZ<sup>27</sup> basis set for  $[\text{Zn}\{\text{Au}_2(\text{dppm})(\text{D-pen})_2\}]$ ,  $[\text{Zn}\{\text{Au}_2(\text{dppm})(\text{L-cys})_2\}]$ ,  $[\text{Zn}\{\text{Au}_2(\text{dppm})(\text{L-cys})(\text{D-pen})\}]$ ,  $[\text{Zn}\{\text{Au}_2(\text{dppe})(\text{D-pen})_2\}]$ ,  $[\text{Zn}\{\text{Au}_2(\text{dppe})(\text{L-cys})_2\}]$ , and  $[\text{Zn}\{\text{Au}_2(\text{dppe})(\text{L-cys})(\text{D-pen})\}]$ . Solvent (methanol) effects were evaluated by using the polarizable continuum model (PCM). The resulting relative free energy in kJ/mol of these molecules is listed in Table S2 (ESI<sup>†</sup>).

#### Single-crystal X-ray structure determination.

The single-crystal X-ray diffraction measurements for **1<sub>Ni</sub>**, **1<sub>Zn</sub>** and **2<sub>Ni</sub>** were performed on a RIGAKU FR-E Superbright rotating-anode X-ray source with a Mo target ( $\lambda = 0.71075 \text{ \AA}$ ) equipped with a RIGAKU RAXIS VII imaging plate as a detector at 200 K. The single-crystal X-ray diffraction measurement for **2<sub>Zn</sub>** was performed at the BL02B1 beamline in SPring-8 with the approval of the Japan Synchrotron Radiation Research Institute (JASRI) with a diffractometer equipped with a Rigaku Mercury 2 CCD detector or a PILATUS3 X CdTe 1M (T = 100 K). The intensity data were collected in  $\omega$  scan mode and were corrected for Lorentz polarization. Empirical absorption corrections were also applied.

The structures of the compounds were solved by direct methods using SHELXS-97 or SHELXS-2014.<sup>28</sup> Structural refinements were carried out using full matrix least-squares (SHELXL-2018).<sup>28</sup> The contribution of solvated water molecules was excluded using the SQUEEZE program.<sup>29</sup> Hydrogen atoms were included in the calculated positions. All non-hydrogen atoms were refined anisotropically. All the phenyl groups were modelled using AFIX instructions. For **1<sub>Ni</sub>** and **1<sub>Zn</sub>**, the coordinate of one of the Au atom was fixed in the final refinement so as to prevent the drift. A global RIGU and several ISOR instructions were used to model the structure. SADI and DFIX restraints were applied for C-N bonds in **2<sub>Ni</sub>** and **2<sub>Zn</sub>**, respectively. The crystal data are summarized in Table S3 (ESI<sup>†</sup>).

## Conclusion

In this study, we showed that the reactions of a 1:1 mixture of L1<sup>P<sup>AP</sup></sup> and L2<sup>P<sup>AP</sup></sup> with M = Ni<sup>II</sup>, Zn<sup>II</sup> selectively produce homoleptic [M(L1<sup>P<sup>AP</sup></sup>)]/[M(L2<sup>P<sup>AP</sup></sup>)] (**1<sub>M</sub>**) for P<sup>AP</sup> = dpmm and heteroleptic [M(L3<sup>P<sup>AP</sup></sup>)] (**2<sub>M</sub>**) for P<sup>AP</sup> = dppe. Thus, the generation of homoleptic versus heteroleptic coordination species was successfully controlled via slight modification of the P<sup>AP</sup> linker, which is ascribed to the directional matching between the [M(L-cys/d-pen)]<sub>2</sub><sup>2-</sup> donor and the [Au<sub>2</sub>(P<sup>AP</sup>)]<sup>2+</sup> acceptor. The present study, which also evidenced appreciable differences in the spectroscopic properties between **1<sub>M</sub>** and **2<sub>M</sub>**, should contribute to the development of multinuclear and metallosupramolecular systems controlled by homolepticity versus heterolepticity.

## Conflicts of interest

There are no conflicts to declare.

## Acknowledgements

This work was supported by JST CREST (Grant No. JPMJCR13L3) and JSPS KAKENHI (Grant Nos. 19K05496 and 18H05344). The synchrotron radiation experiments were performed at BLO2B1 and BLO2B2 of SPring-8 with the approval of JASRI (Proposal Nos. 2018A1502, 2018B1296, 2019A1279 and 2019B1107).

## Notes and references

- L. F. Lindoy, *Coord. Chem. Rev.*, 2008, **252**, 811.
- (a) D. L. Caulder and K. N. Raymond, *J. Chem. Soc., Dalton Trans.*, 1999, 1185-1200; (b) M. Fujita, M. Tominaga, A. Hori and B. Therrien, *Acc. Chem. Res.*, 2005, **38**, 369-378; (c) R. Chakrabarty, P. S. Mukherjee and P. J. Stang, *Chem. Rev.*, 2011, **111**, 6810-6918.
- (a) S. De, K. Mahata and M. Schmittel, *Chem. Soc. Rev.*, 2010, **39**, 1555-1575; (b) M. M. Safont-Sempere, G. Fernández and F. Würthner, *Chem. Rev.*, 2011, **111**, 5784-5814; (c) W. M. Bloch and G. H. Clever, *Chem. Commun.*, 2017, **53**, 8506-8516; (d) S. Pullen and G. H. Clever, *Acc. Chem. Res.*, 2018, **51**, 3052-3064; (e) A. Kobayashi, M. Kato, *Chem. Lett.*, 2017, **46**, 154-162; (f) H. L.-K. Fu, V. W.-W. Yam, *Chem. Lett.*, 2018, **47**, 605-610; (g) C. Kammerer, G. Erbland, Y. Gisbert, T. Nishino, K. Yasuhara and G. Rapenne, *Chem. Lett.*, 2019, **48**, 299-308.
- (a) S. P. Argent, H. Adams, T. Riis-Johannessen, J. C. Jeffery, L. P. Harding and M. D. Ward, *J. Am. Chem. Soc.*, 2006, **128**, 72-73; (b) J.-R. Li, H.-C. Zhou, *Angew. Chem. Int. Ed.*, 2009, **48**, 8465-8468; (c) H. Li, Z.-J. Yao, D. Liu and G.-X. Jin, *Coord. Chem. Rev.*, 2015, **293-294**, 139-157; (d) B. Champin, P. Mobian and J.-P. Sauvage, *Chem. Soc. Rev.*, 2007, **36**, 358-366.
- (a) S. Kusaka, R. Sakamoto, Y. Kitagawa, M. Okumura and H. Nishihara, *Chem. Asian J.*, 2012, **7**, 907-910. (a) V. Leandri, A. R. P. Pizzichetti, B. Xu, D. Franchi, W. Zhang, I. Benesperi, M. Freitag, L. Sun, L. Kloos and J. M. Gardner, *Inorg. Chem.* 2019, **58**, 12167-12177. B. Liu, S. Monroe, Z. Li, M. A. Javed, D. Ramirez, C. G. Cameron, K. Colón, J. Roque III, S. Kilina, J. Tian, S. A. McFarland and W. Sun, *ACS Appl. Bio Mater.*, 2019, **2**, 2964-2977.
- J.-R. Li and H.-C. Zhou, *Nat. Chem.*, 2010, **2**, 893-898.
- F. J. Rizzuto, J. P. Carpenter and J. R. Nitschke, *J. Am. Chem. Soc.*, 2019, **141**, 9087-9095.
- C. Minozzi, A. Caron, J.-C. Grenier-Petel, J. Santandrea and S. K. Collins, *Angew. Chem. Int. Ed.*, 2018, **57**, 5477-5481.
- (a) L. A. Barrios, C. Bartual-Murgui, E. Peyrecave-Lleixà, B. L. Guennic, S. J. Teat, O. Roubeau and G. Aromí, *Inorg. Chem.*, 2016, **55**, 4110-4116; (b) L. Münzfeld, C. Schoo, S. Bestgen, E. Moreno-Pineda, R. Köppe, M. Ruben and P. W. Roesky, *Nat. Commun.*, 2019, **10**, 3135.
- (a) C. Mejuto, G. Guisado-Barrios, D. Gusevb and E. Peris, *Chem. Commun.*, 2015, **51**, 13914-13917; (b) K. Omoto, N. Hosono, M. Gochomori, K. Albrecht, K. Yamamoto and S. Kitagawa, *Chem. Commun.*, 2018, **54**, 5209-5212; (c) S.-Y. Wang, J.-Y. Huang, Y.-P. Liang, Y.-J. He, Y.-S. Chen, Y.-Y. Zhan, S. Hiraoka, Y.-H. Liu, S.-M. Peng and Y.-T. Chan, *Chem. Eur. J.*, 2018, **24**, 9274-9284; (d) R. Zhu, W. M. Bloch, J. J. Holstein, S. Mandal, L. V. Schäfer and G. H. Clever, *Chem. Eur. J.* 2018, **24**, 12976-12982.
- (a) A. Kaeser, M. Mohankumar, J. Mohanraj, F. Monti, M. Holler, J.-J. Cid, O. Moudam, I. Nierengarten, L. Karmazin-Brelot, C. Duhayon, B. Delavaux-Nicot, N. Armaroli and J.-F. Nierengarten, *Inorg. Chem.*, 2013, **52**, 12140-12151; (b) F. Q.-F. Sun, S. Sato and M. Fujita, *Angew. Chem. Int. Ed.*, 2014, **53**, 13510-13513; (c) D. Preston, J. E. Barnsley, K. C. Gordon and J. D. Crowley, *J. Am. Chem. Soc.*, 2016, **138**, 10578-10585; (d) W. M. Bloch, J. J. Holstein, W. Hiller and G. H. Clever, *Angew. Chem. Int. Ed.*, 2017, **56**, 8285-8289; (e) M. Holler, B. Delavaux-Nicot and J.-F. Nierengarten, *Chem. Eur. J.*, 2019, **25**, 4543-4550.
- (a) K. Mahata, M. L. Saha and M. Schmittel, *J. Am. Chem. Soc.*, 2010, **132**, 15933-15935; (b) M. L. Saha and M. Schmittel, *J. Am. Chem. Soc.*, 2013, **135**, 17743-17746.
- (a) D. Volz, M. Wallesch, S. L. Grage, J. Göttlicher, R. Steininger, D. Batchelor, T. Vitova, A. S. Ulrich, C. Heske, L. Weinhardt, T. Baumann and S. Bräse, *Inorg. Chem.*, 2014, **53**, 7837-7847; (b) M. Baskin, N. Fridman, M. Kasa and M. Galia, *Dalton Trans.*, 2017, **46**, 15330-15339.
- (a) A. Igashira-Kamiyama and T. Konno, *Dalton Trans.*, 2011, **40**, 7249-7263; (b) N. Yoshinari and T. Konno, *Bull. Chem. Soc. Jpn.*, 2018, **91**, 790-812.
- N. Yoshinari and T. Konno, *Chem. Rec.*, 2016, **16**, 1647-1663.
- Y. Hashimoto, K. Tsuge and T. Konno, *Chem. Lett.*, 2010, **39**, 601-603.
- A. Igashira-Kamiyama, N. Matsushita, R. Lee, K. Tsuge and T. Konno, *Bull. Chem. Soc. Jpn.*, 2012, **85**, 706-708.
- H. Schmidbaur, A. Wohlleben, F. E. Wagner, O. Orama and G. Huttner, *Chem. Ber.*, 1977, **110**, 1748-1754.
- A pair of asymmetric S atoms in the homoleptic **1<sup>M</sup>** has the *R,S* configuration. On the other hand, that in the heteroleptic **2<sup>M</sup>** adopts the *R,R* configuration for the *A* isomer and the *S,S* configuration for the *C* isomer.

- 20 (a) H. Schmidbaur and A. Schier, *Chem. Soc. Rev.*, 2008, **37**, 1931-1951; (b) H. Schmidbaur, W. Graf and G. Müller, *Angew. Chem. Int. Ed. Engl.*, 1988, **27**, 417-419.
- 21 (a) P. A. Bates and J. M. Waters, *Inorg. Chim. Acta*, 1985, **98**, 125-129; (b) C. K. Mirabelli, D. T. Hill, L. F. Faucette, F. L. McCabe, G. R. Girard, D. B. Bryan, B. M. Sutton, J. O. L. Bartus, S. T. Crooke and R. K. Johnson, *J. Med. Chem.*, 1987, **30**, 2181-2190.
- 22 N. Yoshinari, C. Li, R. Lee, N. Kuwamura, A. Igashira-Kamiyama and T. Konno, *Inorg. Chem.*, 2015, **54**, 8881-8883.
- 23 (a) H. Yamatera, *Bull. Chem. Soc. Jpn.*, 1958, **31**, 95-108; (b) K. Okamoto, K. Wakayama, H. Einaga, S. Yamada, J. Hidaka, *Bull. Chem. Soc. Jpn.*, 1983, **56**, 165-170.
- 24 Y. Hashimoto, N. Yoshinari, D. Naruse, K. Nozaki and T. Konno, *Inorg. Chem.*, 2013, **52**, 14368-14375.
- 25 M. J. Frisch, et al. Gaussian 09, Revision C.01, Gaussian, Inc., Wallingford CT, (2009).
- 26 (a) A. D. Becke, *J. Chem. Phys.*, 1993, **98**, 5648-5652; (b) A. D. Becke, *Phys. Rev. A*, 1988, **38**, 3098-3100; (c) C. Lee, W. Yang, R. G. Parr, *Phys. Rev. B*, 1988, **37**, 785-789.
- 27 (a) P. J. Hay and W. R. Wadt, *J. Chem. Phys.*, 1985, **82**, 270-283; (b) W. R. Wadt and P. J. Hay, *J. Chem. Phys.*, 1985, **82**, 284-298; (c) P. J. Hay and W. R. Wadt, *J. Chem. Phys.*, 1985, **82**, 299-310.
- 28 G. M. Sheldrick, *Acta Cryst.*, 2008, **A64**, 112-113.
- 29 A. L. Spek, *Acta Crystallogra.* 2015, **C71**, 9-18.